



Faculty of Information and Communication Technology

AN EFFICIENT PSYCHOVISUAL THRESHOLD TECHNIQUE IN IMAGE COMPRESSION

Ferda Ernawan

PhD

2014

**AN EFFICIENT PSYCHOVISUAL THRESHOLD TECHNIQUE
IN IMAGE COMPRESSION**

FERDA ERNAWAN

**A thesis submitted
in fulfillment of the requirements for the degree of Doctor of Philosophy**

Faculty of Information and Communication Technology

UNIVERSITI TEKNIKAL MALAYSIA MELAKA

2014

DECLARATION

I declare that this thesis entitled "An Efficient Psychovisual Threshold Technique in Image Compression" is the result of my own research except as cited in the references. The thesis has not been accepted for any degree and is not concurrently submitted in candidature of any other degree.

Signature : 

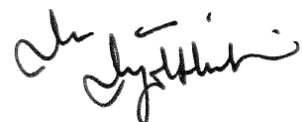
Name : FERDA ERNAWAN

Date : 20 August 2014

APPROVAL

I hereby declare that I have read this thesis and in my opinion this thesis is sufficient in terms of scope and quality for the award of Doctor of Philosophy.

Signature



Supervisor Name

: DR. NUR AZMAN ABU

Date

: 22 August 2014

DEDICATION

I would like to dedicate this thesis to my beloved mother and father

ABSTRACT

Nowadays, psychovisual model plays a critical role in an image compression system. The psychovisual threshold gives visual tolerance to the human visual system by reducing the amount of frequency image signals. The sensitivity of the human eye can be fully explored and exploited in the qualitative experiment by describing what has been seen or by image quality judgment. However, the result of the psychovisual threshold through qualitative experiment depends on the test condition of the human visual systems and through repetitive viewing sessions. In a modern image compression, there is a need to provide some flexibility to obtain quality levels of the image output based on user preferences. The concept of psychovisual threshold is designed to determine quality levels of the image output. The psychovisual threshold represents an optimal amount of frequency image signals in image compression. This research proposes the psychovisual threshold through a quantitative experiment that can automatically predict an optimal balance between image quality and compression rate in image compression. The contribution of its frequency image signals to the image reconstruction will be the primitive of psychovisual threshold in image compression. It is very challenging to develop a psychovisual threshold from the contribution of the frequency image signals for each frequency order. In this research, the psychovisual threshold prescribes the quantization values and bit allocation for image compression. The psychovisual threshold is the basic primitive prior to generating quantization tables in image compression. The psychovisual threshold allows a developer to design adaptively customized quantization values according to his or her target image quality. The psychovisual threshold is also elementary and primitive for generating a set of bit allocation for frequency image signals. A set of bit allocation based on psychovisual threshold assigns the amount of bits for frequency image signals. A set of bit allocation refers to the psychovisual threshold instead of the quantization process in image compression. This research investigates the basic understanding of the psychovisual threshold in image compression. The experimental results provide significant improvement in the image compression. The psychovisual threshold which is presented as quantization tables, customized quantization tables and as a set of bit allocation gives a significant improvement on both of the quality of the image reconstruction and the average bit length of Huffman code. This research shows that psychovisual threshold is practically the best measure for optimal frequency image signals on image compression.

ABSTRAK

Model psikovisual memainkan peranan yang penting dalam sistem pemampatan imej pada hari ini. Ambang psikovisual memberi ketahanan terhadap sistem visual manusia dengan cara mengurangkan jumlah isyarat imej frekuensi. Sensitiviti mata manusia boleh diterokai dan dieksplorasi sepenuhnya melalui eksperimen kualitatif dengan cara menerangkan apa yang mereka telah lihat ataupun membuat penilaian ke atas kualiti imej. Walau bagaimanapun, hasil keputusan ke atas ambang psikovisual yang diperolehi melalui eksperimen kualitatif bergantung kepada keadaan ujian sistem visual manusia melalui sesi pemerhatian yang berulang kali. Dalam pemampatan imej yang moden, fleksibiliti sangat diperlukan bagi mendapatkan hasil akhir imej yang berkualiti mengikut kesesuaian pengguna. Konsep ambang psikovisual telah direka untuk menentukan aras kualiti hasil akhir imej. Ambang psikovisual ini mewakili jumlah optimum isyarat imej frekuensi dalam pemampatan imej. Kajian ini mencadangkan ambang psikovisual melalui eksperimen kuantitatif yang boleh meramal keseimbangan optimum antara kualiti imej dan kadar mampatan dalam sebuah pemampatan imej secara automatik. Isyarat imej frekuensi turut menyumbang untuk pembinaan semula imej yang menjadi kepada asas ambang psikovisual dalam pemampatan imej. Membangunkan ambang psikovisual daripada dapatan isyarat imej frekuensi bagi setiap aturan frekuensi merupakan satu cabaran. Dalam kajian ini, ambang psikovisual ditetapkan nilai pengkuantuman dan sejumlah bit untuk pemampatan imej. Ambang psikovisual merupakan asas utama bagi menghasilkan jadual pengkuantuman dalam pemampatan imej dan membolehkan pengguna merekabentuk nilai-nilai asas pengkuantuman adaptif yang boleh berubah mengikut kualiti imej sasaran. Ambang psikovisual juga menjadi asas kepada penghasilan sejumlah set bit untuk isyarat imej frekuensi. Penentuan sejumlah set bit ini berdasarkan kepada ambang psikovisual yang memberikan jumlah bit untuk isyarat imej frekuensi. Sejumlah set bit merujuk kepada ambang psikovisual dan menggantikan proses pengkuantuman dalam pemampatan imej. Kajian ini menyelidik asas ambang psikovisual dalam pemampatan imej. Keputusan kajian menunjukkan terdapat peningkatan yang ketara dalam pemampatan imej. Ambang psikovisual ditunjukkan dalam bentuk jadual kuantisasi, jadual kuantisasi reka bentuk khusus dan sejumlah set bit untuk memberi peningkatan yang ketara pada kedua-dua kualiti pembinaan semula imej dan purata panjang bit kod Huffman. Kajian ini menunjukkan bahawa ambang psikovisual adalah ukuran terbaik mengoptimalkan isyarat imej frekuensi dalam pemampatan imej.

ACKNOWLEDGEMENT

In preparing this thesis, I would like to express my full gratitude to my first supervisor, Dr. Nur Azman Abu for his guidance, patience, critics and friendship throughout the years of my Ph.D study at Universiti Teknikal Malaysia Melaka. His advice and motivation has always been resourceful and enlightening. I am also very thankful to my second supervisor, Professor Dr. Nanna Suryana for his encouragement and continued support during my research study. Without their continued support and interest, this thesis would not have been possible.

I am indebted to the Ministry of Education, Malaysia for giving me a funding during the course of this research through the Fundamental Research Grant Scheme (FRGS) (FRGS/2012/FTMK/SG05/03/1/F00141). Besides, I am also indebted to Universiti Teknikal Malaysia Melaka (UTeM) for providing me the assistance to endure my Ph.D study. My sincere appreciation is also extended to all my friends at the Faculty of Information and Communication Technology, UTeM who have assisted me at various occasions during my research. My fellow graduates and postgraduate students in UTeM are also acknowledged for their continued support.

Additionally, I would like to convey my thanks to Dr. Ir. Edi Noersasongko the rector of Universitas Dian Nuswantoro (UDINUS) for providing me financial support at the initial stage of my study. Then, I would also thank Dr. Kusni Ingih the vice rector of UDINUS and Dr. Abdul Syukur the Dean, Faculty of Computer Science UDINUS for encouraging and motivating me to complete this study on time.

Finally, I would like to express my personal gratitude to my parents and my brothers for their continuous encouragement. Thank you and may Allah bless you all.

TABLE OF CONTENTS

	PAGE
DECLARATION	
APPROVAL	
DEDICATION	
ABSTRACT	i
ABSTRAK	ii
ACKNOWLEDGEMENT	iii
TABLE OF CONTENTS	iv
LIST OF TABLES	ix
LIST OF FIGURES	xi
LIST OF APPENDICES	xvii
LIST OF SYMBOLS	xviii
LIST OF PUBLICATIONS	xix
CHAPTER	
1. INTRODUCTION	1
1.0 Introduction	1
1.1 Problem Background	2
1.2 Problem Statement	4
1.3 Research Questions	5
1.4 Research Objectives	6
1.5 Research Scopes	8
1.6 Research Contributions	9
1.7 Thesis Structure Organization	9
1.8 Summary	12
2. LITERATURE REVIEW ON IMAGE COMPRESSION	14
2.0 Introduction	14
2.1 A Brief Overview of Image Compression	15
2.2 A Brief Overview of JPEG and JPEG2000	17
2.2.1 JPEG Compression	18
2.2.2 JPEG2000	20

2.3 Lossless Image Compression	22
2.4 The Psychovisual Redundancy in Image Compression	23
2.5 Recent of Quantization Table Generation Around the Globe	24
2.6 Specific Application of Quantization Tables	28
2.7 Research Directions on The Quantization Process of Image Compression	29
2.8 Anatomy of The Human Audibility	32
2.9 Overview of The Psychoacoustic Model	32
2.10 Overview of The Audio Coding	35
2.11 Anatomy of The Human Visibility	37
2.12 Overview of The Psychovisual Threshold	38
2.13 Psychophysical Adjustment Methods	40
2.14 Frequency Order of The Image Signals	41
2.15 Procedure of Image Compression Steps And Apparatus	42
2.15.1 Colour Transformation From RGB to YCbCr colour	43
2.15.2 Mathematical Transform	44
2.15.2.1 Discrete Cosine Transform (DCT)	44
2.15.2.2 Discrete Wavelet Transform (DWT)	48
2.15.2.3 Discrete Orthogonal Tchebichef Moment	49
2.15.2.4 Discrete Orthonormal Tchebichef Moment	56
2.15.3 Quantization Process	59
2.15.3.1 JPEG Quantization Tables Design	60
2.15.3.2 Tchebichef Moment Quantization Tables	64
2.15.4 Dequantization	67
2.15.5 Zigzag Pattern	67
2.15.6 Differential Pulse Code Modulation of DC Coefficients	68
2.15.7 Run-Length Encoding of The AC Coefficients	69
2.15.8 Entropy Coding	70
2.16 A Brief Overview of The Extended JPEG Image Compression	71
2.17 The Customized Quantization Tables for Extended JPEG Image Compression	72
2.18 Quality Measurement of Image Compression	74
2.19 Summary	76
3. RESEARCH METHODOLOGY	77
3.0 Introduction	77

3.1 Research Phases	77
3.1.1 Phase 1: Background Study of The Psychovisual Threshold in Image Compression	79
3.1.2 Phase 2: Study on The Principle of The Psychoacoustic Model and The Concept of Audio Coding	82
3.1.3 Phase 3: Analysis on How to Generate A Psychovisual Threshold	84
3.1.4 Phase 4: Design of The Psychovisual Threshold to The Quantization Process	86
3.1.5 Phase 5: Design of The Psychovisual Threshold to The Bit Allocation	89
3.1.6 Phase 6: Develop An Image Compression to Evaluate The Effectiveness of The Psychovisual Threshold	92
3.1.7 Phase 7: Validate and Report on The Results	94
3.2 Image Sources	95
3.3 Experimental Setup	97
3.3.1 A Psychovisual Threshold Experiment to Generate The Optimal Quantization Tables for Image Compression	97
3.3.2 An Adaptive Psychovisual Threshold Experiment to Generate The Customized Quantization Tables for Image Compression	99
3.3.3 Development of A Set of Bit Allocation Based on The Psychovisual Threshold for Image Compression	100
3.4 Evaluation of The Psychovisual Threshold for Image Compression	101
3.4.1 The Average Bit Length of Huffman's Code	102
3.4.2 The Image Quality Measurement	103
3.5 Summary	104
4. DEVELOPMENT OF THE PSYCHOVISUAL THRESHOLD	105
4.0 Introduction	105
4.1 Development of The Optimal Quantization from The Psychovisual Threshold	106
4.1.1 The Psychovisual Threshold on Small Discrete Cosine Transform	107
4.1.2 An Optimal DCT Quantization Tables From The Psychovisual Threshold	110
4.1.3 The Psychovisual Threshold on Small Discrete Tchebichef Moment	113
4.1.4 An Optimal TMT Quantization Table From The Psychovisual Threshold	116
4.1.5 The Psychovisual Threshold on Large Discrete Cosine Transform	119
4.1.6 The Large DCT Quantization Table Generation From The Psychovisual Threshold	121
4.1.7 The Psychovisual Threshold on Large Discrete Tchebichef Moment Transform	125

4.1.8 The Large TMT Quantization Table Generation From The Psychovisual Threshold	127
4.2 Development of The Customized Quantization Tables From The Psychovisual Threshold	130
4.2.1 The Scaling Psychovisual Threshold on Discrete Cosine Transform	130
4.2.2 The Adaptively Customized DCT Quantization Tables From The Scaling Psychovisual Threshold	132
4.2.3 The Scaling Psychovisual Threshold on Discrete Tchebicichef Moment Transform	134
4.2.4 The Adaptively Customized TMT Quantization Tables From The Scaling Psychovisual Threshold	136
4.3 Development of A Set of Bit Allocation Based on The Psychovisual Threshold	137
4.3.1 Local Bit Allocation on The AC Coefficients	137
4.3.1.1 A Set of Bit Allocation on The Short Blocks of AC Coefficients	138
4.3.1.2 A Set of Bit Allocation on The Medium Blocks of AC Coefficients	140
4.3.1.3 A Set of Bit Allocation on The Long Blocks of AC Coefficients	141
4.3.2 Probability Density Function of The AC Coefficients	143
4.3.2.1 Probability Density Function of The Peak AC Coefficients	143
4.3.2.2 Probability Density Function of The Non-Peak AC Coefficients	144
4.4 Summary	145
5. EXPERIMENTAL RESULTS	146
5.0 Introduction	146
5.1 The Experiments of The Psychovisual Threshold Schemes	147
5.1.1 An Experiment on The Impact of The Psychovisual Threshold to The Quantization Process	148
5.1.2 An Experiment on The Performance of The Psychovisual Threshold to The Customized Quantization Tables	149
5.1.3 An Experiment on The Effect of The Psychovisual Threshold to The Bit Allocation	150
5.2 The Average Bit Length of Huffman Code From The Psychovisual Threshold Schemes	150
5.2.1 The Average Bit Length of Huffman Code From An Optimal Quantization Process	151
5.2.2 The Average Bit Length of Huffman Code From Customized Quantization Tables	159

5.2.3 The Average Bit Length of Huffman Code From A Set of Bit Allocation	162
5.2.3.1 Histograms of The Peak AC Coefficients	165
5.2.3.2 Probability Density Function of The Peak AC Coefficients	166
5.2.3.3 Histogram of The Non-Peak AC Coefficients	168
5.2.3.4 Probability Density Function of The Non-Peak AC Coefficients	169
5.3 The Quality of Image Reconstruction From The Psychovisual Threshold Schemes	171
5.4 The Average File-Size of The Output Image From The Psychovisual Threshold Schemes	177
5.5 The Average Compression Ratio of Image Compression From The Psychovisual Threshold Schemes	179
5.6 The Visual Quality of the Image Outputs From The Psychovisual Threshold Schemes	182
5.6.1 The Visual Quality of the Image Output From The Psychovisual Threshold on Small and Large Discrete Transform	183
5.6.2 The Visual Quality of the Image Output From Adaptive Psychovisual Threshold	188
5.6.3 The Visual Quality of the Image Output From Bit Allocation Based on The Psychovisual Threshold	195
5.7 Discussion on The Experimental Results	204
5.7.1 Discussion on The Experimental Results From An Optimal Quantization Process	205
5.7.2 Discussion on The Experimental Results From Customized Quantization Tables	207
5.7.3 Discussion on The Experimental Results From A Set of Bit Allocation	209
5.8 Summary	210
6. CONCLUSION	212
6.0 Introduction	212
6.1 Research Accomplishment	212
6.2 Research Contributions	214
6.3 Limitation of The Research Study	216
6.4 Future Research	217
6.5 Conclusion	219
REFERENCES	221
APPENDICES	241

LIST OF TABLES

TABLE	TITLE	PAGE
2.5	Research groups in the current quantization table generation	24
2.6	The recent of quantization table generation for specific image processing applications	28
2.7	The strengths and weaknesses of the psychovisual techniques in image compression	30
2.15.2.3a	The squared-norm of the scaled Tchebichef polynomials for $N=8$.	51
2.15.2.3b	The kernel matrix value of 8×8 orthogonal Tchebichef polynomials	53
4.1.6a	The index of quantization values on each frequency order	122
4.1.6b	The DCT quantization values on each frequency order for luminance	123
4.1.6c	The DCT quantization values on each frequency order for chrominance	124
4.1.8a	The TMT quantization values on each frequency order for luminance	127
4.1.8b	The TMT quantization values on each frequency order for chrominance	128
4.3.1.1a	A set of bit allocation on the local frequency blocks of 8 coefficients on 256×256 DCT for luminance (left) and chrominance (right)	139
4.3.1.1b	A set of bit allocation on the local frequency blocks of 8 coefficients on 256×256 TMT for luminance (left) and chrominance (right)	139
4.3.1.2a	A set of bit allocation on the local frequency blocks of 16 coefficients on 256×256 DCT for luminance (left) and chrominance (right)	140
4.3.1.2b	A set of bit allocation on the local frequency blocks of 16 coefficients on 256×256 TMT for luminance (left) and chrominance (right)	141

4.3.1.3a	A set of bit allocation on the local frequency blocks of 32 coefficients on 256×256 DCT for luminance (left) and chrominance (right)	142
4.3.1.3b	A set of bit allocation on the local frequency blocks of 32 coefficients on 256×256 TMT for luminance (left) and chrominance (right)	142
5.2.1a	The average bit length of Huffman code from JPEG image compression for 40 real images	152
5.2.1b	The average bit length of Huffman code from JPEG image compression for 40 graphical images	153
5.2.1c	The average bit length of Huffman code from TMT image compression for 40 real images	155
5.2.1d	The average bit length of Huffman code from TMT image compression for 40 graphical images	155
5.2.2a	Average bit length of Huffman code from customized quantization tables for high compression rate	160
5.2.2b	Average bit length of Huffman code from customized quantization tables for medium compression rate	160
5.2.2c	Average bit length of Huffman code from customized quantization tables for low compression rate	161
5.2.3a	The average bit length of Huffman code from a set of bit allocation on the local frequency block of 8, 16 and 32 coefficients based on the psychovisual threshold for JPEG image compression	163
5.2.3b	The average bit length of Huffman code from a set of bit allocation on the local frequency blocks of 8, 16 and 32 coefficients based on the psychovisual threshold for TMT image compression	163
5.3a	The average quality of image reconstruction from JPEG image compression for 40 real images and 40 graphical images	172
5.3b	The average quality of image reconstruction from TMT image compression for 40 real images and 40 graphical images	173
5.3c	The average quality of image reconstruction from adaptive image compression for 40 real images and 40 graphical images	175
5.4a	The average file-size of the compressed image using DCT and TMT for 40 real images and 40 graphical images	177
5.4b	The average file-size of the adaptive compressed image using customized quantization tables from the scaling psychovisual threshold	178
5.5a	The average compression ratio from the psychovisual threshold schemes for 40 real images and 40 graphical images	180
5.5b	The average compression ratio from the adaptive psychovisual threshold schemes for 40 real images and 40 graphical images	181

LIST OF FIGURES

FIGURE	TITLE	PAGE
1.7	Structural flow of the thesis.	10
2.1	General image compression scheme	16
2.9	The absolute hearing threshold under quiet condition [Chen and Yu, 2005]	33
2.15.2.1a	The first four 8×8 DCT of set $C_n(x)$ for $n = 0, 1, 2, 3$ [Abu et. al., 2010]	45
2.15.2.1b	8×8 DCT basis function [Hunt and Mukundan, 2004]	46
2.15.2.1c	The first four 256×256 DCT of set $C_n(x)$ for $n = 0, 1, 2, 3$	47
2.15.2.2	Wavelet decomposition structure	48
2.15.2.3a	The first four discrete orthogonal 8×8 Tchebichef polynomials $t_n(x)$ for $n = 0, 1, 2$ and 3 [Abu et. al., 2010]	54
2.15.2.3b	Visual representation of the TMT block matrices	54
2.15.2.3c	8×8 TMT basis function [Hunt and Mukundan, 2004]	55
2.15.2.4	The first four discrete 256×256 Tchebichef polynomials $t_n(x)$ for $x=0, 1, 2$ and 3	59
2.15.3.1a	The visualization of JPEG quantization table for luminance	62
2.15.3.1b	The visualization of JPEG quantization table for chrominance	63
2.15.3.2a	The visualization of TMT quantization table for luminance	66
2.15.3.2b	The visualization of TMT quantization table for chrominance	66
2.15.5	Zigzag order under regular of 8×8 discrete transform	68
3.1	The research framework consists of seven phases	78
3.1.1	Illustration of the background to the study	80

3.1.2	Illustration of the literature review	82
3.1.3	Illustration of the analysis phase	85
3.1.4	Illustration of the research design	87
3.1.5	Zigzag order under regular of 256×256 discrete transform	90
3.1.6	Illustration of the testing and implementation	93
3.1.7	Illustration of the validation and evaluation	94
4.1.1a	Average reconstruction error of incrementing DCT coefficients on 8×8 DCT luminance for 40 real images	108
4.1.1b	Average reconstruction error of incrementing DCT coefficients on 8×8 DCT chrominance for 40 real images	108
4.1.2a	The visualization of an optimal 8×8 DCT quantization table for luminance	111
4.1.2b	The visualization of an optimal 8×8 DCT quantization table for chrominance	111
4.1.2c	The visualization of JPEG quantization table from the psychovisual threshold for luminance.	112
4.1.2d	The visualization of JPEG quantization table from the psychovisual threshold for chrominance.	112
4.1.3a	Average reconstruction error of incrementing TMT coefficients on 8×8 TMT luminance for 40 real images	114
4.1.3b	Average reconstruction error of incrementing TMT coefficients on 8×8 TMT chrominance for 40 real images	114
4.1.4a	The visualization of an optimal 8×8 TMT quantization table for luminance	117
4.1.4b	The visualization of an optimal 8×8 TMT quantization table for chrominance	117
4.1.4c	The visualization of TMT quantization table from the psychovisual threshold for luminance	118
4.1.4d	The visualization of TMT quantization table from the psychovisual threshold for chrominance	118
4.1.5	Average reconstruction error of incrementing DCT coefficients on 256×256 DCT luminance and chrominance for 40 real images	120
4.1.6	The finer 256×256 DCT quantization tables for luminance and chrominance	125
4.1.7	Average reconstruction error of incrementing TMT coefficients on 256×256 TMT luminance and chrominance for 40 real images	126
4.1.8	The finer 256×256 TMT quantization tables for luminance and chrominance	129

4.2.1a	Average reconstruction error from the scaling DCT psychovisual threshold with $SF = -25, 0$ and 25 on 8×8 DCT luminance for 40 real images	131
4.2.1b	Average reconstruction error from the scaling DCT psychovisual threshold with $SF = -25, 0$ and 25 on 8×8 DCT chrominance for 40 real images	131
4.2.3a	Average reconstruction error from the scaling TMT psychovisual threshold with $QS = -25, 0$ and 25 on 8×8 TMT luminance for 40 real images	135
4.2.3b	Average reconstruction error from the scaling TMT psychovisual threshold with $QS = -25, 0$ and 25 on 8×8 TMT chrominance for 40 real images	135
4.3.2.2	Standard normal distribution function with $\mu = 0$ and $\sigma^2 = 1$	144
5.1.1	Image compression consists of two-dimensional 8×8 DCT	148
5.1.2	Adaptive image compression consists of two-dimensional 8×8 DCT	149
5.1.3	Image compression using a set of bit allocation consists of two-dimensional 256×256 DCT	150
5.2.1a	The visualization on the average bit length of Huffman code from DCT psychovisual threshold schemes on AC luminance for 40 real images and 40 graphical images	154
5.2.1b	The visualization on the average bit length of Huffman code from TMT psychovisual threshold schemes on AC luminance for 40 real images and 40 graphical images	156
5.2.1c	Histograms of the AC luminance using 8×8 default JPEG quantization tables (i), 8×8 TMT quantization tables (ii), 8×8 DCT psychovisual threshold (iii), 8×8 TMT psychovisual threshold (iv), 256×256 DCT psychovisual threshold (v) and 256×256 TMT psychovisual threshold (vi) for 40 real images	157
5.2.1d	Histograms of the AC chrominance using 8×8 default JPEG quantization tables (i), 8×8 TMT quantization tables (ii), 8×8 DCT psychovisual threshold (iii), 8×8 TMT psychovisual threshold (iv), 256×256 DCT psychovisual threshold (v) and 256×256 TMT psychovisual threshold (vi) for 40 real images	158
5.2.2	The visualization on the average bit length of Huffman code from the scaling psychovisual threshold on AC luminance for 40 real images	161
5.2.3	The visualization on the average bit length of Huffman code from a set of bit allocation on AC luminance for 40 real images	164
5.2.3.1a	Histograms of the peak AC luminance for local frequency blocks of 8 coefficients on 256×256 DCT (left) and 256×256 TMT (right) for 40 real images	165

5.2.3.1b	Histograms of the peak AC chrominance for local frequency blocks of 8 coefficients on 256×256 DCT (left) and 256×256 TMT (right) for 40 real images	165
5.2.3.2a	The extreme distribution of the peak AC luminance (i), the peak AC chrominance (iii) on 256×256 DCT and the extreme distribution of the peak AC luminance (ii), the peak AC chrominance (iv) on 256×256 TMT for local frequency blocks of 8 coefficients on 40 real images	166
5.2.3.2b	The probability density function of the peak AC luminance (i), the peak AC chrominance (iii) on 256×256 DCT and the probability density function of the peak AC luminance (ii), the peak AC chrominance (iv) on 256×256 TMT for local frequency blocks of 8 coefficients on 40 real images	167
5.2.3.3	Histograms of the non-peak AC luminance (i), the non-peak AC chrominance (iii) on 256×256 DCT and histograms of the non-peak AC luminance (ii), the non-peak AC chrominance (iv) on 256×256 TMT for local frequency blocks of 8 coefficients on 40 real images	168
5.2.3.4	Probability density function of the non-peak AC luminance (i), the non-peak AC chrominance (iii) on 256×256 DCT and probability density function of the non-peak AC luminance (ii), the non-peak AC chrominance (iv) on 256×256 TMT for local frequency blocks of 8 coefficients on 40 real images	170
5.3a	The visualization on the average reconstruction error from a set of bit allocation on the local frequency blocks of 8, 16 and 32 coefficients for 40 real images	174
5.3b	The visualization on the average quality of image reconstruction from a set of bit allocation on the local frequency blocks of 8, 16 and 32 coefficients for 40 real images	174
5.3c	The visualization on the average quality of image reconstruction from the scaling psychovisual threshold for 40 real images	176
5.4a	The visualization on the average file-size of the compressed image from the psychovisual threshold schemes for 40 real images	178
5.4b	The visualization on the average file-size of the compressed image from the scaling psychovisual threshold for 40 real images	179
5.5a	The visualization on the average compression ratio from the psychovisual threshold schemes for 40 real images	180
5.5b	The visualization on the average compression ratio from the scaling psychovisual threshold for 40 real images	181
5.6	The original Baboon image (i) and the original Lena image (ii)	182
5.6.1a	The comparison of visual outputs between the original Baboon image (i), JPEG quantization table (ii), 8×8 DCT psychovisual threshold (iii) and 256×256 DCT psychovisual threshold (iv) zoomed in to 800%	184

5.6.1b	The comparison of visual outputs between the original Baboon image (i), TMT quantization table (ii), 8×8 TMT psychovisual threshold (iii) and 256×256 TMT psychovisual threshold (iv) zoomed in to 800%	185
5.6.1c	The comparison of visual outputs between the original Lena image (i), JPEG quantization table (ii), 8×8 DCT psychovisual threshold (iii) and 256×256 DCT psychovisual threshold (iv) zoomed in to 800%	186
5.6.1d	The comparison of visual outputs between the original Lena image (i), TMT quantization table (ii), 8×8 TMT psychovisual threshold (iii) and 256×256 TMT psychovisual threshold (iv) zoomed in to 800%	187
5.6.2a	The comparison of visual outputs between the original Baboon image (i), JPEG quantization table with $QF = 25$ (ii), DCT psychovisual threshold with $SF = 25$ (iii) and TMT psychovisual threshold with $QS = 25$ (iv) zoomed in to 800%	189
5.6.2b	The comparison of visual outputs between the original Lena image (i), JPEG quantization table with $QF = 25$ (ii), DCT psychovisual threshold with $SF = 25$ (iii) and TMT psychovisual threshold with $QS = 25$ (iv) zoomed in to 800%	190
5.6.2c	The comparison of visual outputs between the original Baboon image (i), JPEG quantization table with $QF = 50$ (ii), DCT psychovisual threshold with $SF = 0$ (iii) and TMT psychovisual threshold with $QS = 0$ (iv) zoomed in to 800%	191
5.6.2d	The comparison of visual outputs between the original Lena image (i), JPEG quantization table with $QF = 50$ (ii), DCT psychovisual threshold with $SF = 0$ (iii) and TMT psychovisual threshold with $QS = 0$ (iv) zoomed in to 800%	192
5.6.2e	The comparison of visual outputs between the original Baboon image (i), JPEG quantization table with $QF = 75$ (ii), DCT psychovisual threshold with $SF = -25$ (iii) and TMT psychovisual threshold with $QS = -25$ (iv) zoomed in to 800%	193
5.6.2f	The comparison of visual outputs between the original Lena image (i), JPEG quantization table with $QF = 75$ (ii), DCT psychovisual threshold with $SF = -25$ (iii) and TMT psychovisual threshold with $QS = -25$ (iv) zoomed in to 800%	194
5.6.3a	The comparison of visual outputs between the original Baboon image (i), the results of bit allocation on the local blocks of 8 coefficients (ii), 16 coefficients (iii) and 32 coefficients (iv) on 256×256 DCT zoomed in to 800%	196

5.6.3b	The original Baboon image (i) and the differentiate visual outputs of bit allocation from the original Baboon image with multiply by a factor of 4 on the local blocks of 8 coefficients (ii), 16 coefficients (iii) and 32 coefficients (iv) on 256×256 DCT zoomed in to 800%	197
5.6.3c	The comparison of visual outputs between the original Baboon image (i), the results of bit allocation on the local blocks of 8 coefficients (ii), 16 coefficients (iii) and 32 coefficients (iv) on 256×256 TMT zoomed in to 800%	198
5.6.3d	The original Baboon image (i) and the differentiate visual outputs of bit allocation from the original Baboon image with multiply by a factor of 4 on the local blocks of 8 coefficients (ii), 16 coefficients (iii) and 32 coefficients (iv) on 256×256 TMT zoomed in to 800%	199
5.6.3e	The comparison of visual outputs between the original Lena image (i), the results of bit allocation on the local blocks of 8 coefficients (ii), 16 coefficients (iii) and 32 coefficients (iv) on 256×256 DCT zoomed in to 800%	200
5.6.3f	The original Lena image (i) and the differentiate visual outputs of bit allocation from the original Lena image with multiply by a factor of 16 on the local blocks of 8 coefficients (ii), 16 coefficients (iii) and 32 coefficients (iv) on 256×256 DCT zoomed in to 800%	201
5.6.3g	The comparison of visual outputs between the original Lena image (i), the results of bit allocation on the local blocks of 8 coefficients (ii), 16 coefficients (iii) and 32 coefficients (iv) on 256×256 TMT zoomed in to 800%	202
5.6.3h	The original Lena image (i) and the differentiate visual outputs of bit allocation from the original Lena image with multiply by a factor of 16 on the local blocks of 8 coefficients (ii), 16 coefficients (iii) and 32 coefficients (iv) on 256×256 TMT zoomed in to 800%	203

LIST OF APPENDICES

APPENDIX	TITLE	PAGE
A	Sample Input of 40 Real Images and 40 Graphical Images	241
B	Histograms of the Frequency AC Coefficients	245
C	Image Reconstruction Error	264

LIST OF SYMBOLS

AC	-	Alternative Coefficient
ACY	-	Alternative Coefficient Luminance Y
ACCb	-	Alternative Coefficient Chrominance Cb
ACCr	-	Alternative Coefficient Chrominance Cr
DC	-	Direct Coefficient
DCY	-	Direct Coefficient Luminance Y
DCCb	-	Direct Coefficient Chrominance Cb
DCCr	-	Direct Coefficient Chrominance Cr
EOB	-	End-of-Block
NACY	-	Non-Peak Alternative Coefficient Luminance Y
NACCb	-	Non-Peak Alternative Coefficient Chrominance Cb
NACCr	-	Non-Peak Alternative Coefficient Chrominance Cr
PACY	-	Peak Alternative Coefficient Luminance Y
PACCb	-	Peak Alternative Coefficient Chrominance Cb
PACCr	-	Peak Alternative Coefficient Chrominance Cr
QF	-	Quality Factor
QS	-	Quality Scale
SF	-	Scaling Factor

LIST OF PUBLICATIONS

- N.A. Abu, F. Ernawan, N. Suryana and S. Sahib, (2013). Image Watermarking Using Psychovisual Threshold over the Edge. *Information and Communication Technology*, pp. 519-527.
- N.A. Abu, F. Ernawan and S. Sahib, (2013). Psychovisual Model on Discrete Orthonormal Transform. *International Conference on Mathematical Sciences and Statistics (ICMSS 2013)*, 5-7 February 2013, Kuala Lumpur, Malaysia, pp. 309-314.
- N.A. Abu, F. Ernawan and N. Suryana, (2013). A Generic Psychovisual Error Threshold for the quantization table generation on JPEG Image Compression. *9th International Colloquium on Signal Processing and its Applications (CSPA 2013)*, 8 - 10 March 2013, Kuala Lumpur, Malaysia, pp. 39-43.
- F. Ernawan, N.A. Abu and N. Suryana, (2013). TMT Quantization Table Generation Based on Psychovisual Threshold for Image Compression. *International Conference of Information and Communication Technology (ICoICT 2013)*, 20-22 March 2013, Bandung, Indonesia, pp. 202-207.
- F. Ernawan, N.A. Abu and N. Suryana, (2013). Adaptive Tchebichef Moment Transform Image Compression Using Psychovisual Model. *Journal of Computer Science*, Vol. 9, No. 6, pp. 716-725.
- F. Ernawan, N.A. Abu and N. Suryana, (2014). An Adaptive JPEG Image Compression Using Psychovisual Model. *Advanced Science Letters*, Vol. 20, No. 1, pp. 026-031.
- F. Ernawan, N.A. Abu and N. Suryana, (2014). An Optimal Tchebichef Moment Quantization Using Psychovisual Threshold for Image Compression. *Advanced Science Letters*, Vol. 20, No. 1, pp. 070-074.
- F. Ernawan, N.A. Abu and N. Suryana, (2014). Integrating A Smooth Psychovisual Threshold Into An Adaptive JPEG Image Compression. *Journal of Computers*, Vol. 9, No. 3. pp. 644-653.
- F. Ernawan, N.A. Abu and N. Suryana, (2014). A Psychovisual Threshold for Generating Quantization Process in Tchebichef Moment Image Compression. *Journal of Computers*, Vol. 9, No. 3, pp. 702-710.